Organic Geochemical Characterization of Crude Oils from Western Sirt Basin, Libya.

Alsharef A. Albaghdady
Department of Geology, Faculty of Science /Sebha University, Libya
Corresponding Author: als.albaghdady@sebhau.edu.ly

Abstract   The Sirt Basin contains most of Libya's producing oil fields. It is located in northern Libya, south of the Gulf of Sirt in the Mediterranean Sea. The main aim of this study is to determine the type of organic matter, depositional conditions of the source rocks and thermal maturity of the crude oil based on organic geochemical parameters. The organic geochemical analyses were determined by gas chromatography (GC) and gas chromatography/mass spectrometry (GC/MS). Six crude oil samples were collected from the Ghani and En Naga oil fields in the western Sirt Basin. The results suggest that all of the oils are derived from source rocks rich in marine organic matter deposited under oxic to suboxic saline conditions. Based on biomarker ratios such as pristane/phytane, isoprenoids/n-alkanes, carbon preference index (CPI), 22S/22S+22R homohopane ratio, diasteranes/steranes, gammacerane index, C29 20S/20S+20R, C29/C30 hopanes and Ts/Ts+Tm, which are used as source and correlation parameters, it proposed that these oils are in early mature stage and could be sourced from similar marine shale except for one sample which may indicate more salinity of source rocks.
Keywords: (Biomarker, crude oil, organic matter Sirt Basin, thermal maturity)

<div dir="rtl">

الخصائص الجيوكيميائية العضوية لعينات من النفط الخام من غرب حوض سرت، ليبيا

الشارف عبدالسلام البغدادي

قسم علوم الأرض– كلية العلوم– جامعة سبها، ليبيا

للمراسلة:als.albaghdady@sebhau.edu.ly

الملخص يعد حوض سرت من اهم الاحوض الرسوبية في ليبيا واكثرها انتاجا، ويقع هذا الحوض شمال ليبيا وجنوب خليج سرت. تهدف هذه الدراسة الى تحديد نوعية المادة العضوية والظروف البيئية لصخور المصدر والنضوج الحراري لخام الزيت بالحوض اعتمادا على المعاملات الجيوكيميائية العضوية. قد اجريت التحاليل الجيوكيميائية بواسطة الغاز كروماتوجرافيا (GC) Gas Chromatography و الغاز كروماتوجرافيا (GC-MS) Gas Chromatography-Mass Spectrometry الموصل بجهاز تحليل طيف الكتلة. استخدمت في هذه الدراسة ست عينات من الزيت الخام التي جمعت من حقل الغاني وحقل الناقة الواقعين في منخفض زلة غرب حوض سرت. وبينت النتائج ان جميع عينات الزيت تولدت من مادة عضوية توضعت في بيئة بحرية مالحة ومؤكسجة. وبالاعتمادا على المعاملات مثل Pr/Ph (pristane/phytane), isoprenoids/n-alkanes, carbon preference index (CPI), 22S/22S+22R homohopane ratio (C32 αβ homohopane 22S/ C32 αβ- homohopane 22S + 22R), 27Dia/27R (C27 βα-diasterane 20S/C27 ααα-sterane 20R), G/C31R (gammacerane/ C31 αβ homohopane 22R), C29 20S/20S+20R (C29 ααα-sterane 20S/C29 ααα-sterane 20S + 20R), C30βα/C30αβ (C30 βα-hopane /C30 αβ-hopane) and Ts/Ts+Tm (C27 18α(H)-22,29,30-trisnorneohopane/ C27 18α(H)-22,29,30-trisnorneohopane + C27 17α(H)-22,29,30-trisnorhopane), التي استخدمت كمعملات لتحديد صخر المصدر والمظاهاة، بينت الدراسات المعملية ان صخر المصدر بلغ مرحلة النضوج المبكر، كما ان ان معظم عينات الزيت المأخوذة اُنتجت من صخر مصدر واحد وهو الطين الصفحي البحري فيما عدا عينة واحدة اظهرت صخر مصدر توضع في ظروف اكثر ملوحة مقارنة ببقية العينات.

الكلمات المفتاحية: Biomarker ، النفط الخام ، المواد العضوية حوض سرت ، النضج الحراري .

</div>

1.Introduction

Crude oils contain a huge number of organic compounds that can be connected to their original organisms during deposition of the rocks. Organic geochemists are commonly used these biological markers to classify groups of genetically connected crude oils to the depositional environments [1, 2]. The Sirt Basin is the sixth largest hydrocarbon producing province in the world, with oil and gas reserves estimated at 33 to 45 billion barrels of oil equivalent (BBOE; [3]. It contains most of the hydrocarbon reserves and most producing oil fields in Libya, and approximately 29% of Africa's total reserves [4]. In the Sirt Basin, oil is more abundant than gas. The oils have approximately 32 to 44 API gravity and sulfur content of 0.15 to 0.66% [5]. These oils are found in sandstone and limestone reservoirs ranging in age from Cambrian to Tertiary. Although the organic geochemistry of crude oils in the Sirt Basin has been studied in detail especially in eastern of the basin [6, 7], little information is available regarding the western part of the Basin In this study, some of crude oil samples from Ghani and En Naga oilfields are investigated to identify the thermal maturity, age, organic type

and depositional environment of source rocks from western Sirt Basin, Libya.

1.1 Regional Setting:

The Sirt Basin is located in northern part of Libya and stretches southward from the Gulf of Sirt and covers an approximate area of 600000 km2 across central Libya [8]. The Zallah Trough is located between the Waddan Uplift in the west and the Az Zahrah-Al Hufrah platform on the east (Fig.1). The Zallah Trough narrows northwards and becomes shallower to form the Dur al Abd Trough. These toughs separate the Az Zahrah-Al Hufrah Platform from the Waddan Uplift in the area of the Mabrouk Field. The Zallah Trough also extends southwards to connect with the Abu Tumayam Trough and narrows to the east to connect with the Al Kotlah Graben in the region of the Dur Mansour and Al Kuf oil fields [9]. Generally, Sirt Basin contains a succession of marine clastic and carbonate sediments reaching a maximum thickness of approximately 7500 m [10]. Sirt Basin represents a continental rift area and part of the Tethyan rift system [11, 12]. During much of the Paleozoic and Mesozoic, there was an uplifted sirt arch with NW-SE orientation [13]. This uplifted arch experienced a rifting phase that began in the Late Cretaceous [13]. Non-marine Nubian sediment began to accumulate in grabens in the Early Cretaceous Period [9, 13]. Due to a full-scale rifting and block faulting in the Late Cretaceous Period, marine transgressions and related facies changes across contemporaneous faults occurred in the basin [9]. In the Late Tertiary, see level rise and consequently all the platforms were covered by sediments. During the Oligocene Period and the early Miocene Period, intense tectonic activity resumed. Finally, at the end of the mid-Miocene Period the present onshore part of the Sirt Basin had emerged [14]. The structure of the Sirt Basin generally consists of large numbers of platforms and troughs that forms mainly northwest-southeast, east-west and northeast-southwest arms with extended faults [15, 16]; Fig.1). According to the type of the structures; shale, mainly deposited in troughs and carbonate formed on platforms which resulted in complex stratigraphy on the Basin. Sedimentary succession thicknesses in the basin vary in the troughs and platforms, ranging from 1500 to 7000 m [17] and represent deposits from the Cambrian to Tertiary [18]. Cambro-Ordovician sediment is distributed widely in the basin. The Triassic and Jurassic sediments are deposited more in the northeastern part of the basin, while the Lower Cretaceous sediments are located more in the southeastern part of the basin. The Upper Cretaceous marine sequence is the largest sequence in the basin, ranging in age from Cenomanian to Maastrichtian with the thickest sediments found in the troughs [9]. Fig. (2) illustrates the stratigraphic section in central Sirt Basin.
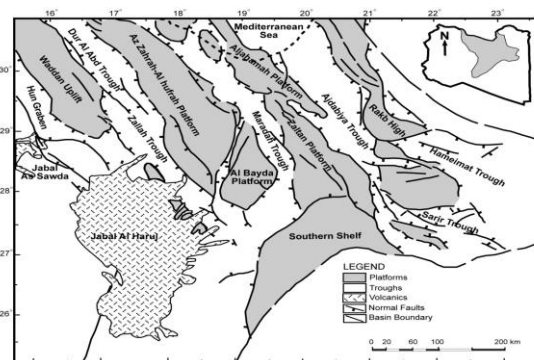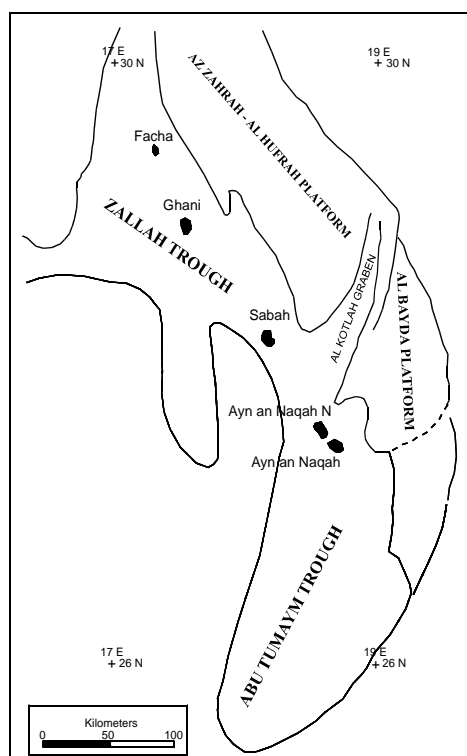

Fig. 1: Map shows location and the structural elements of the Sirt Basin (modified after Abadi et al, 2008)
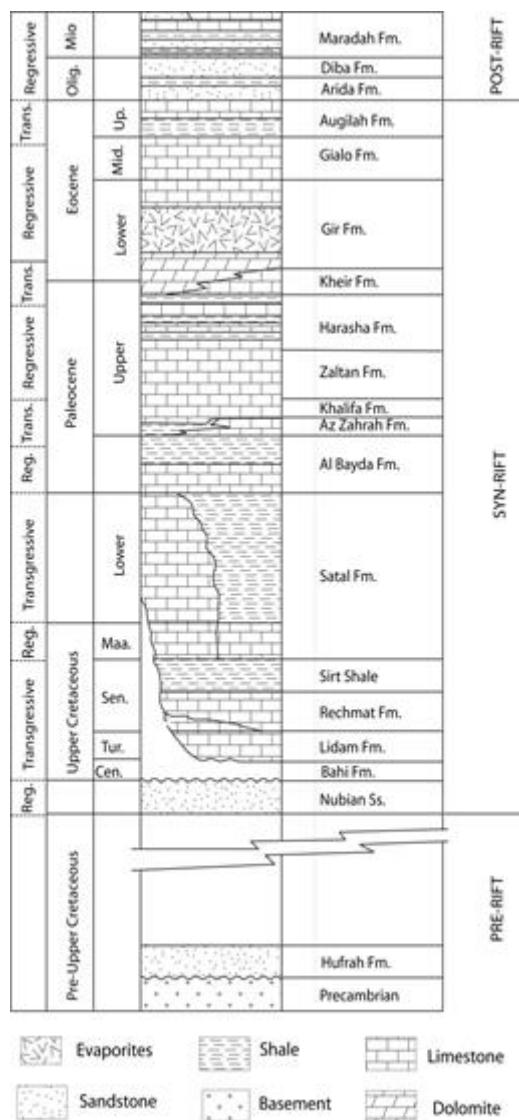
Fig. 2: Stratigraphic section of the central Sirt Basin (modified after Ahlbrandt, 2001)

2. xperimental: MethodsSix of crude oil samples used in this study were collected from the Ghani and En Naga oil fields in the western Sirt Basin. Figure 3 shows the location of the two oil fields. For each oil sample, Asphaltenes was removed by precipitation with n-pentane. The crude oils were

dissolved by adding 1 ml of dichloromethane and transferred into a small glass vial. The volume of the samples was increased by adding 40 ml of n-pentane and was stored in a refrigerator for 12 hours in order to precipitate the asphaltenes. The suspended asphaltene was separated by centrifuging for 20 minutes at 1000 RPM. pressure. The saturate fraction was dissolved in a small volume of n-hexane and loaded into the column. The saturate hydrocarbon vial was then rinsed with n-hexane and also transferred to the top of the column. Three bed volumes of hexane were added to insure complete separation of the branched and cyclic compounds from the n-alkanes. The gas chromatography (GC) used for analyzing the saturate fractions was a Hewlett Packard 6890 coupled with flame ionization detector (GC/FID) equipped with an Agilent J&W DB-Petro column (100 m x 0.25 mm 0.5 μm film thickness). The samples were injected using a splitless injector and helium used as the carrier gas. The oven was initially maintained at 40°C for 1.5 min; subsequently temperatures were programmed from 40 to 300°C at 4°C/min and held isothermal for 14 min. The injector and detector temperatures were kept at 300°C. An Agilent 7890A gas chromatography interfaced with a 5975C mass selective detector (MSD) and equipped with an Agilent J&W 60 m x 0.25 μm DB-5MS fused silica capillary column was used for the analysis. 1μl of fraction solution in dichloromethane was injected into the column.

subsequent temperatures were programmed from 40 to 300°C at 4°C/min and held isothermal for 14 min. The injector and detector temperatures were kept at 300°C. The column was linked directly to the ion source through a transfer line operated at 300°C; the electronic impact ion source was operated at 70 eV. Data were acquired in a selected ion monitoring (SIM) mode and processed with the Hewlett Packard Chemstation software.

3. Results and Discussion
3.1. Source Input and Depositional Condition
3.1.1. n-Alkane and Isoprenoid
The n-Alkane distributions in crude oils and source rocks may reflect the origin of the organic matter of the source [19]. GC performed on saturate fraction of Sirt Basin oil shows a normal alkane distribution range from C_{12} to C_{35} maximizing at C_{16} and C_{17}, which is indicating that the oil samples have marine algal origin. The n-alkane distributions in representative oil samples obtained from the studied fields of the Sirt Basin show generally similar carbon number distribution (Fig. 4; Table 1).
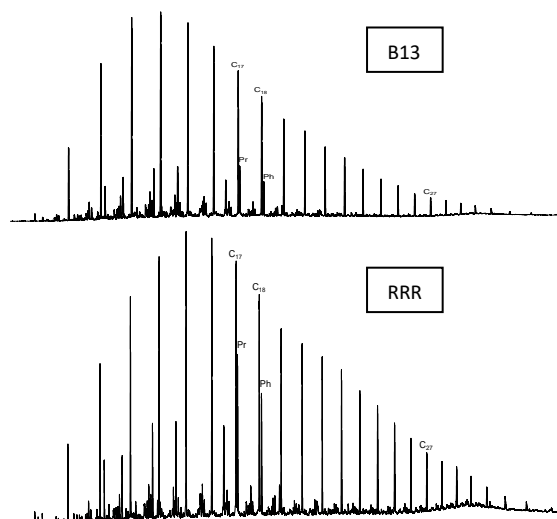
Fig. 4: Distribution of n-alkanes and isoprenoid from oil samples of the En Naga (B13) and Ghani (R23) oil fields.

Fig. 3: Map shows the location of the oil fields included in this study.

The samples were injected using a splitless injector and helium used as the carrier gas. The oven was initially maintained at 40°C for 1.5 min,

The n-alkane distribution and carbon number distribution curve of normalized C_{10} to C_{33} n-alkanes show that the oils are dominated by low molecular weight compounds and the high molecular weight n-alkanes are less abundant, which may suggest that these oils are derived from kerogen deposited in marine environments. The pristane/phytane ratio is commonly used as an indicator of redox conditions in the depositional environment of organic matter [20, 21]. During oxic condition, the phytol side-chain of chlorophyll is believed to form pristane, while under anoxic conditions, phytane is produced. All oil groups in this study show pristane/phytane ratios between 1.17 and 1.36 which may suggest oxic to suboxic condition for the depositional environment [2, 22].The low Pr/nC_{17} and Ph/nC_{18} ratios range from 0.40 to 0.74 and 0.36 to 0.75, respectively in non-biodegraded samples. These

values suggest deposition in an open marine environment [23]. A plot of Pr/nC_{17} versus Ph/nC_{18} can be used to indicate the type of organic matter (Fig. 5). The distribution of samples on this plot suggests a marine environment for organic matter within the rocks.

Table 1: N-alkanes and isoprenoids parameters.

Sample	Pr/Ph	Pr/C$_{17}$	Ph/C$_{18}$	C$_{17}$/C$_{27}$	CPI
B-13	1.34	0.40	0.38	0.13	1.17
B-16	1.36	0.41	0.36	0.15	1.14
GG-12	1.17	0.55	0.52	0.22	1.04
RRR-19	1.32	0.53	0.50	0.19	1.12
RRR-23	1.20	0.74	0.75	0.24	1.12
RRR-31	1.32	0.59	0.54	0.22	1.12

Pr/Ph = pristane/phytane; Pr/C17 = pristane/n-heptadecane; Ph/C18 = phytane/n-octadecane; CPI = Carbon Preference Index; C17/C27 = n-heptadecane/C27 normal alkane.
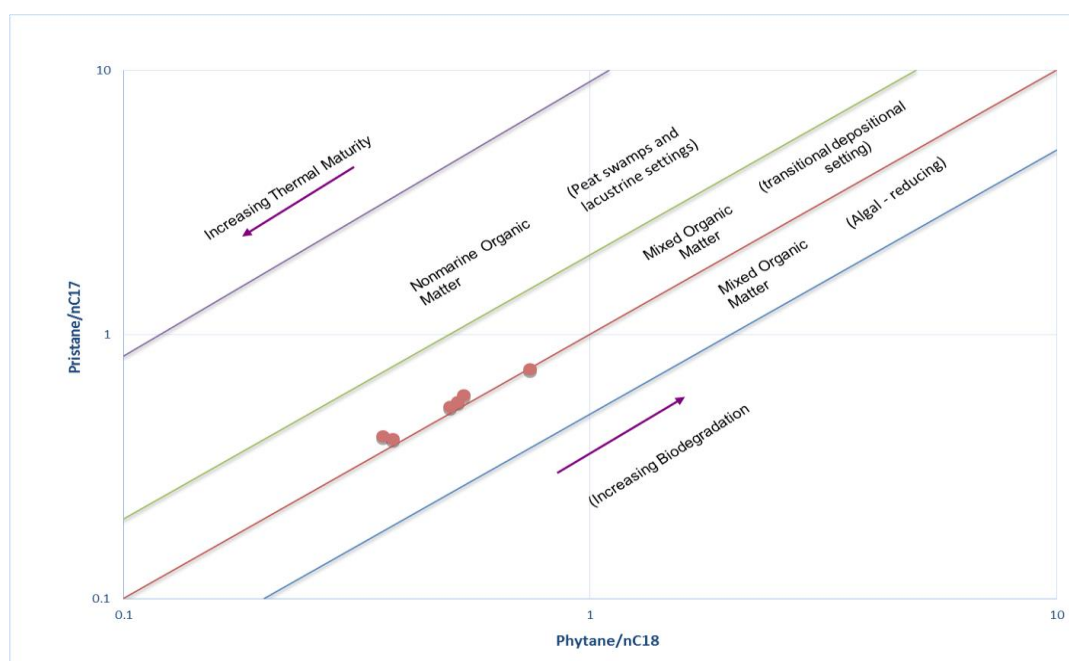
Fig. 5: Plot of Pr/nC_{17} vs. Ph/nC_{18} of crude oils used in this study.

3.1.2. Terpane Parameters:

In this study, crude oil samples from Sirt Shale have different terpane distributions among the different oil groups (Fig. 6; Table 2 for identification). All crude oil samples have similar terpane distributions and show a high number of hopanes than tricyclic terpanes which may indicate that they have similar organic matter type. Table 3 shows the terpane parameters which used in this study. High C$_{35}$ homohopanes is an indicator of oxic marine conditions during deposition which is reflected in the 22R+22S C35/(C$_{31}$-C$_{35}$) homohopane ratio. This ratio is used to estimate the redox conditions of the depositional environment of the source [24, 25]. These ratios studied in all samples are very low, ranging from 0.08 to 0.13 which may indicate oxic conditions in the depositional environment. This is consistent with the conditions suggested by high pristane/phytane ratios. In the studied samples, C$_{29}$ and C$_{30}$ 17α (H)-hopanes, the two

most abundance terpanes and the C$_{29}$/C$_{30}$ hopane ratios between 0.47 and 0.61 may indicate the clay-bearing character of the source rocks G/C$_{31}$R homohopane ratio ranges from 0.34 to 0.55 which may indicate less saline environment but one sample 3R-23 has ratio of 0.83 indicating more salinity [1, 26]. The oil samples show low abundance of C$_{24}$ tetracyclic terpanes which could be used as a characteristic of clastic marine depositional environments since a high abundance of C$_{24}$ tetracyclic has been reported to be associated with a high input of terrestrially derived organic matter [27] and carbonate [28, 29, 30, 31] and evaporate [29, 31] depositional environments. However, the sample RRR-23 has also relatively high C$_{24}$ tetracyclic which may indicate higher saline environment than others. The ratios of C$_{23}$ tricyclic to C$_{30}$ hopane range from 0.47 to 0.61 and support the nature of the marine environment.

3.1.3. Sterane Parameters:

Figure 7 shows the distribution of steranes for all groups (see Table 4 for peak identifications and Table 5 for steranes-diasteranes parameters). The relative abundance of C_{27}, C_{28} and C_{29} steranes have been found to be a good indicator for organic matter type. All of the studied samples show a high abundance of C_{27} steranes that are believed to be derived from marine organic matter (phytoplankton) and a relatively low abundance of C_{29} steranes indicate a low contribution from higher plant organic matter evident in the high ratios of C_{27}/C_{29} steranes [32, 33]. The presence of C_{30} steranes in the studied crude oil samples strongly indicates marine organic matter for these rocks. The ratio of $C_{28}/C_{29}\alpha\alpha$ steranes is considered to be parameter to estimate the age of oils in marine settings as it increases from Precambrian to Tertiary due to the relative increase of C_{28} steranes and the decrease of C_{29} steranes through geological time. A ratio of less than 0.5 suggests oils from Lower Paleozoic age and older while ratios between 0.4 and 0.7 for oils of Upper Paleozoic to Lower Jurassic age, and oils with a ratio greater than 0.7 indicate Upper Jurassic to Tertiary oils [34, 35]. In the studies, this ratio ranges from 1.03 to 1.08 which suggests they could be generated from Upper cretaceous source rocks and the sample B-13 has ratio of 0.71 which indicates older source rock age. C_{27} Diasteranes/ C_{27} R regular steranes ratios are generally high in most of oil samples which can be an additional indicator of rich clay content in the source rocks [1].
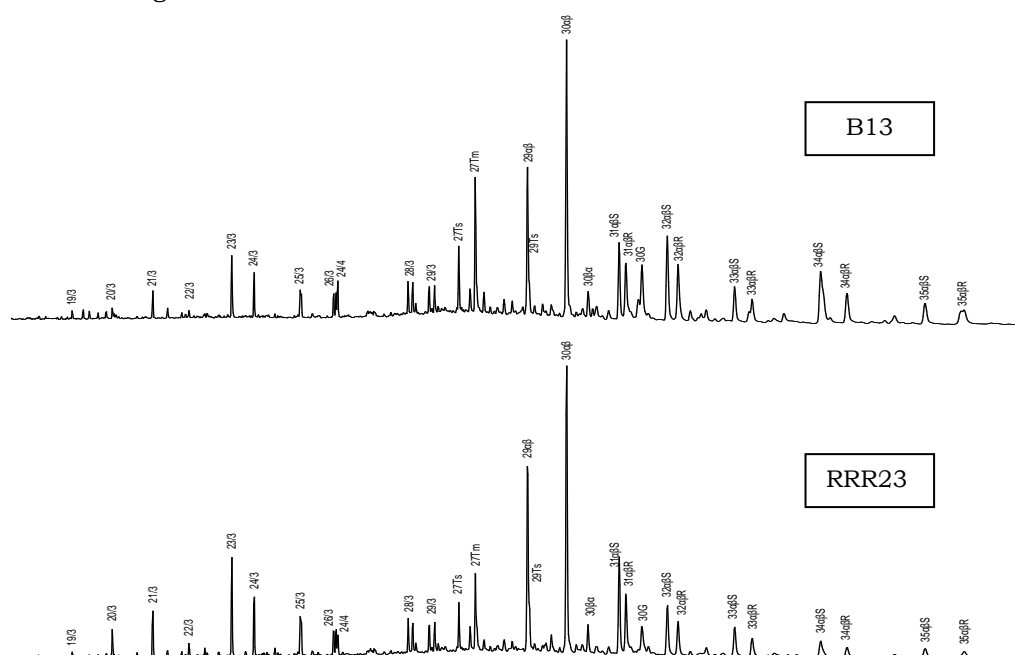
Fig. 6: Terpane distribution of the samples from the En Naga oilfields and the Ghani oilfields.

Table 2: Identifications of tricyclic, tetracyclic and pentacyclic triterpanes.

19/3	C_{19} Tricyclic terpane	29Ts	18α Neonorhopane [C_{29}Ts]
20/3	C_{20} Tricyclic terpane	30αβ	Hopane [C_{30}]
21/3	C_{21} Tricyclic terpane	30βα	17β21α Moretane [C_{30}]
22/3	C_{22} Tricyclic terpane	31αβS	22S Homohopane [C_{31}]
23/3	C_{23} Tricyclic terpane	31αβR	22R Homohopane [C_{31}]
24/3	C_{24} Tricyclic terpane	30G	Gammacerane [C_{30}]
25/3	C_{25} Tricyclic terpane	32αβS	22S Bishomohopane [C_{32}]
26/3	C_{26} [22S] Tricyclic terpane + C_{26} [22R] Tricyclic terpane	32αβR	22R Bishomohopane [C_{32}]
24/4	C_{24} Tetracyclic terpane	33αβS	22S Trishomohopane [C_{33}]
28/3	C_{28} [22S] Tricyclic terpane + C_{28} [22R] Tricyclic terpane	33αβR	22R Trishomohopane [C_{33}]
29/3	C_{29} [22S] Tricyclic terpane + C_{29} [22R] Tricyclic terpane	34αβS	22S Tetrakishomohopane [C_{34}]
27Ts	18α Trisnorneohopane [C_{27} Ts]	34αβR	22R Tetrakishomohopane [C_{34}]
27Tm	17α Trisnorneohopane [C_{27} Tm]	35αβS	22S Pentakishomohopane [C_{35}]
29αβ	Norhopane [C_{29}]	35αβR	22R Pentakishomohopane [C_{35}]

Table 3: Terpane Parameters.

Sample	Ts/ (Ts+Tm)	22S/ (22S+22R)	C23Tr/ C30αβ	C30βα/ C30αβ	C29/C30	C24Tri/ C23Tri	24Tet/ 24Te+26Tri	C35/ (C31-C35)	G/C31R
B-13	0.36	0.55	0.15	0.10	0.50	0.72	0.41	0.13	0.83
B-16	0.46	0.57	0.31	0.09	0.47	0.71	0.22	0.08	0.38
GG-12	0.52	0.56	0.23	0.10	0.49	0.60	0.25	0.12	0.34
RRR-19	0.43	0.57	0.24	0.10	0.47	0.65	0.25	0.10	0.37
RRR-23	0.40	0.57	0.22	0.10	0.61	0.66	0.26	0.09	0.55
RRR-31	0.62	0.54	0.26	0.12	0.47	0.63	0.22	0.08	0.34

Ts/(Ts+Tm) = ratio of C_{27} 18α(H)-22,29,30-trisnorneohopane/ C_{27} 18α(H)-22,29,30trisnorneohopane + C_{27} 17α(H)-22,29,30-trisnorhopane; 22S/(22S+22R) = ratio of C_{32} αβ homohopane 22S/ C32 αβ- homohopane 22S + 22R; C_{23}Tr/C30αβ = C_{23} tricyclic terpane /C_{30} αβ-hopane; C30βα/C30αβ = C_{30} βα-hopane /C_{30} αβ-hopane; C_{29} αβ/C30αβ = ratio of C_{29} αβ-hopane / C_{30} αβ-hopane; C_{24}Tr/C23Tr = C_{24} tricyclic terpane /C_{23} tricyclic terpane; C24Te/24Tet + 26Tet = C_{24} tetracyclic terpane/ 24 tetracyclic terpane +26 tetracyclic terpane; C_{35}/ sum of C_{31}–C_{35} homohopanes; G/C31R= gammacerane/ C_{31} αβ homohopane 22R)
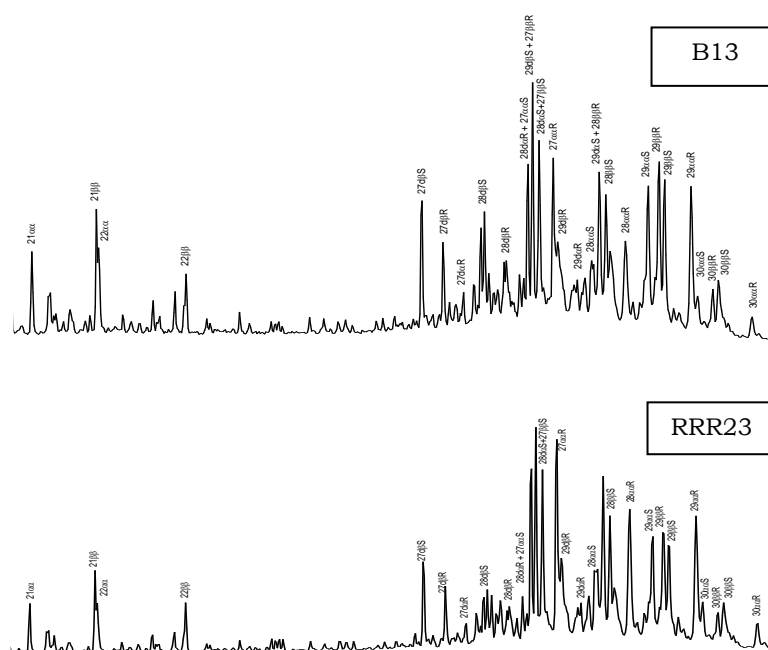
Fig. 7: Sterane distribution from oil samples of the En Naga and the Ghani oil fields.

Table 4: Identifications of steranes and diasteranes.

21αα	Diapregnane	29dαR	24-ethyl-13α(H), 17β(H), 20(R)- diacholestane
21ββ	5α(H), 14β(H), 17β(H) Pregnane	28ααS	24-methyl-5α(H), 14α(H), 17α(H), 20(S)-cholestane
22αα	Diahomopregnane	29dαS + 28ββS	24-ethyl-13α(H), 17β(H), 20(S)- diacholestane + 24-methyl-5α(H), 14β(H), 17β(H), 20(R)-cholestane
22ββ	5α(H), 14β(H), 17β(H) Homopregnane	28ββS	24-methyl-5α(H), 14β(H), 17β(H), 20(S)-cholestane
27dβS	13β (H), 17α(H), 20(S)- diacholestane	28ααR	24-methyl-5α(H), 14α(H), 17α(H), 20(R)-cholestane
27dβR	13β(H), 17α(H), 20(R)- diacholestane	29ααS	24-ethyl-5α(H), 14α(H), 17α(H), 20(S)-cholestane
27dαR	13α(H), 17β(H), 20(R)- diacholestane	29ββR	24-ethyl-5α(H), 14β(H), 17β(H), 20(R)-cholestane
28dβS	24-methyl-13β(H), 17α(H), 20(S)- diacholestane	29ββS	24-ethyl-5α(H), 14β(H), 17β(H), 20(S)-cholestane
28dβR	24-methyl-13β(H), 17α(H), 20(R)- diacholestane	29ααR	24-ethyl-5α(H), 14α(H), 17α(H), 20(R)-cholestane
28dαR + 27ααS	24-methyl-13α(H), 17β(H), 20(R)- diacholestane + 5α(H), 14α(H), 17α(H), 20(S)-cholestane	30ααS	24-propyl-5α(H), 14α(H), 17α(H), 20(S)-cholestane
29dβS + 27ββR	24-ethyl-13β(H), 17α(H), 20(S)- diacholestane + 5α(H), 14β(H), 17β(H), 20(R)-cholestane	30ββR	24-propyl-5α(H), 14β(H), 17β(H), 20(R)-cholestane
28dαS + 27ββS	24-methyl-13α(H), 17β(H), 20(S)- diacholestane + 5α(H), 14β(H), 17β(H), 20(S)-cholestane	29ββS	24-propyl-5α(H), 14β(H), 17β(H), 20(S)-cholestane
27ααR	5α(H), 14α(H), 17α(H), 20(R)-cholestane	30ααR	24-propyl-5α(H), 14α(H), 17α(H), 20(R)-cholestane
29dβR	24-ethyl-13β(H), 17α(H), 20(R)- diacholestane		

Table 5: steranes and diasteranes parameters.

Sample	20S/(20S+20R)	$\beta\beta/(\beta\beta\beta+\alpha\alpha)$	Dia/27R	Pre/27R	27R/29R	28R/29R	%27R	%28R	%29R
B-13	0.48	0.52	0.84	0.45	1.08	0.71	38.78	25.39	35.83
B-16	0.45	0.60	1.16	1.01	1.16	1.07	35.86	33.17	30.97
GG-12	0.49	0.55	0.89	0.52	1.18	1.08	36.15	33.09	30.76
RRR-19	0.48	0.53	0.94	0.67	1.26	1.04	38.16	31.45	30.38
RRR-23	0.47	0.45	0.92	0.26	1.27	1.03	38.37	31.34	30.30
RRR-31	0.48	0.49	0.91	0.58	1.21	1.05	37.09	32.22	30.68

20S/(20S+20R) = C_{29} $\alpha\alpha\alpha$-sterane 20S/C_{29} $\alpha\alpha\alpha$-sterane 20S + 20R; $\beta\beta/(\beta\beta+\alpha\alpha)$ = C_{29} $\alpha\beta\beta$-sterane 20S+20R/C_{29} $\alpha\alpha\alpha$ + $\alpha\beta\beta$-sterane 20S + 20R; 27Dia/27R = C_{27} $\beta\alpha$-diasterane 20S/C_{27} $\alpha\alpha$-sterane 20R; 27R/29R = C_{27} $\alpha\alpha$-sterane 20R /C_{29} $\alpha\alpha$-sterane 20R.28R/29R = C_{28} $\alpha\alpha$-sterane 20R /C_{29} $\alpha\alpha$-sterane 20R; Preg/27R = C_{21} pregnane/C_{27} $\alpha\alpha$-sterane 20R; %27R = percentage of C_{27} $\alpha\alpha$ 20R to sum C_{27}, C_{28}, C_{29} $\alpha\alpha$ 20R steranes; %28R = percentage of C_{28} $\alpha\alpha$ 20R to sum C_{27}, C_{28}, C_{29} $\alpha\alpha$ 20R steranes; %29R = percentage of C_{29} $\alpha\alpha$20Rto sum C_{27}, C_{28}, C_{29} $\alpha\alpha$ 20R steranes.

3.2. Thermal Maturity

3.2.1. Terpane Biomarker Parameters: Both moretanes and hopanes are used to estimate the level of thermal maturity of the oil and source rock [1]. In this study the Moretane/ Hopane ratio is low, 0.09 and 0.12 indicating that the source rocks are mature. The values of the Ts/(Ts+Tm) ratio values range from 0.36 to 0.62 for all oil groups. This biomarker could be influenced by either maturity or source type. The ratios 22S/(22S+22R) of hopane of the samples range from 0.54 to 0.57 indicating that these samples have reached the oil generation window. Peters et al. (2005) proposed that samples containing ratios in the range of 0.50 to 0.54 have barely entered the oil generation window [2] while ratios of 0.57 to 0.62 indicate the main phase of generation that has been reached or surpassed [1].

3.2.2. Sterane Biomarker Parameters: The ratio of 20S/(20S+20R) is the most common used steranes to estimate the level of maturity for oil and source rock. The biologically produced form 20R decreases with increasing maturity while 20S increases with increasing of the maturity. The equilibrium between the two forms is reached within the range of 0.52 and 0.55 where changes in maturity can be observed [1, 36, 37]. The studied samples have values from 0.45 to 49 which indicate that equilibrium values have not been reached. The relative abundance of $C_{29}\beta\beta$ to $C_{29}\alpha\alpha$ is another maturity parameter and this ratio is more reliable when using higher levels of maturity than 20S/ (20S+20R) ratios [2]. The oils exhibit moderate values of ($\beta\beta/(\beta\beta + \alpha\alpha)$) ratios, ranging from 0.45 to 0.60 that do not reach equilibrium. This ratio can be influenced by several factors such as heating rate, presence of clay minerals, the nature of the source material and the depositional environment [38] or lithology [39, 40].

4. Conclusions: The depositional environment and type of organic matter of crude oil samples show generally marine characteristics. Pristane/phytane ratios suggest a depositional environment for the organic matter deposited under oxic to suboxic marine condition. The high abundance of low molecular weight n-alkanes of crude oils supports a high contribution of marine organic matter. The high ratios of C_{27}/C_{29} steranes and occurrence of C_{30} steranes strongly support the marine organic matter contributions. Geochemical parameters suggest that the lithology of the source rocks of these oils is shale and most likely Upper Cretaceous in age with an exception of one sample representing an older age, suggesting at least two sources of oil. These crude oils are generally thermally mature within oil window. The thermal maturity is reflected in the low ratios of moretane/C_{30} hopane. The high maturity for this unit also can be seen in the C_{29} sterane isomerization, Ts/(Ts +Tm), C_{23} tricyclic terpanes /C_{30} Hopane, C_{24} tetracyclic terpanes/C_{23} tricyclic terpanes, 22S/(22S+22R) ratios for C_{31} and C_{32} hopanes and aromatic hydrocarbons.

References

[1]- Peter, K. E., and Moldowan, J. M. "The biomarker guide: interpreting molecular fossils in petroleum and ancient sediments," Englewood Cliffs, New Jersey (1993).

[2]- Peters, K. E., Walters, C. C., and Moldowan, J. M. The Biomarker Guide, Vol. 1 and 2. pp. 1155. Cambridge University Press, Cambridge (2005).

[3]- Macgregor, D. S., and Moody, R. T. J. Mesozoic and Cenozoic petroleum systems of North Africa. In "Petroleum Geology of North Africa" (D. S. Macgregor, R. T. J. Moody and D. D. Clark-Lowes, eds.), pp. 201-216. Geological Society, London, Special Publications No.132 (1998).

[4]- Chatellier, J. Y., and Slevin, A. Review of African petroleum and gas deposits. Journal of African Earth Science 7, 561-578 (1988).

[5]- Parsons, M. G., Zagaar, A. M., and Curry, J. J. Hydrocarbon occurrences in the Sirte Basin, Libya. (A. D. Miall, ed.), pp. 723-732. Canadian Society of Petroleum Geologists Memoir 6 (1980).

[6]- Burwood, R., Redfern, J., and Cope, M. Geochemical evaluation of East Sirte Basin (Libya) petroleum systems and oil provenance. Geological Society, London, Special Publications 207, 203-240 (2003).

[7]- Aboglila, S., Grice, K., Trinajstic, K., Dawson, D., and Williford, K. H. Use of biomarker distributions and compound specific isotopes of carbon and hydrogen to delineate hydrocarbon characteristics in the East Sirte

Basin (Libya). Organic Geochemistry 41, 1249-1258 (2010).

[8]- Ahlbrandt, T. S. "The Sirte Basin Province of Libya: Sirte-Zelten Total Petroleum System," US Department of the Interior, US Geological Survey Bulletin 2202–F (2001).

[9]- Hallett, D. (2002). Petroleum geology of Libya, Elsevier Science.

[10]- Abadi, A. M., van Wees, J. D., van Dijk, P. M., and Cloetingh, S. A. P. L. Tectonics and subsidence evolution of the Sirt Basin, Libya. American Association of Petroleum Geologists Bulletin 92, 993-1027 (2008).

[11]- Futyan, A., and Jawzi, A. H. The hydrocarbon habitat of the oil and gas fields of north Africa with emphasis on the Sirt Basin. In "The geology of the Sirt Basin: Amsterdam, Elsevier" (M. J. Salem, A. S. El-Hawat and A. M. Sbeta, eds.), Vol. 2, pp. 287-307(1996).

[12]- Guiraud, R., and Bosworth, W. Senonian basin inversion and rejuvenation of rifting in Africa and Arabia: synthesis and implications to plate-scale tectonics. Tectonophysics 282, 39-82 (1997).

[13]- Selley, R. C.,. The Sirt basin of Libya. In "African basins: Sedimentary basins of the World" (R. C. Selley, ed), 3, 27– 37 (1997).

[14]- Bu-Argoub, M. F. Palynological and playnofacies studies of the Upper Cretaceous sequence in well C275-65, Sirt Basin, northeast, Libya. In "The geology of the Sirt Basin" (M. T. B. M. J. Salem, A. A. Misallati, and M. A. Sola, ed.), Vol. 1, pp. 419-454. Elsevier, Amsterdam (1996).

[15]- Hallett, D., and El Ghoul, A. Oil and gas potential of the deep trough areas in the Sirt Basin, Libya. In "The geology of Sirt Basin" (M. J. Salem, A. S. El-Hawat and A. M. Sbeta, eds.), Vol. 2, pp. 455-484. Elsevier, Amsterdam (1996).

[16]- Anketell, J. M Structural history of the Sirt Basin and its relationships to the Sabratah Basin and Cyrenaican platform, northern Libya. In "Geology of the Sirt Basin" (M. J. Salem, A. S. El-Hawat and A. M. Sbeta, eds.), Vol. 3, pp. 57-88. Elsevier, Amsterdam (1996).

[17]- Goudarzi, G. H. Structure-Libya. In "The geology of Libya", Vol. 3, pp. 879-892. Academic Press, London (1980).

[18]- Tawadros, E. Geology of Egypt and Libya: Balkema, Rotterdam. Elsevier, 468p (2001).

[19]- Volkmann, J. K. Biological marker compounds as indicators of the depositional environments of petroleum source rocks. In "Lacustrine petroleum source rocks" (A. J. Fleet, K. Kelts and M. R. Talbot, eds.), Vol. 40, pp. 103-122. Geological Society, London, Special Publications (1988).

[20]- Powell, T., and McKirdy, D. Relationship between ratio of pristane to phytane, crude oil composition and geological environment in Australia. Nature 243, 37-39 (1973).

[21]- Didyk, B., Simoneit, B., Brassell, S. C., and Eglinton, G. Organic geochemical indicators of palaeoenvironmental conditions of sedimentation. Nature 272, 216-222 (1978).

[22]- Hunt, J. M. "Petroleum geochemistry and geology " 2/Ed. W. H. Freeman and Company New York (1996).

[23]- Lijmbach, W. On the Origin of Petroleum. In "proceeding 9th world petroleum congress 2", pp. 357-369. Applied Science Publishers, London (1975).

[24]- Peters, K. E., and Moldowan, J. M. Effects of source, thermal maturity, and biodegradation on the distribution and isomerization of homohopanes in petroleum. Organic Geochemistry 17, 47-61 (1991).

[25]- Ahmed, M., Volk, H., Allan, T. and Holland, D.,. Origin of oils in the Eastern Papuan Basin, Papua New Guinea. Organic Geochemistry, 53 137–152 (2012).

[26]- Sinninghe Damsté, J. S., Kenig, F., Koopmans, M. P., Köster, J., Schouten, S., Hayes, J., and de Leeuw, J. W. Evidence for gammacerane as an indicator of water column stratification. Geochimica et Cosmochimica Acta 59, 1895-1900 (1995).

[27]- Philp, R. P., and Gilbert, T. Biomarker distributions in Australian oils predominantly derived from terrigenous source material. Organic Geochemistry 10, 73-84 (1986).

[28]- Zumberge, J. E. Source rocks of the La Luna Formation (Upper Cretaceous) in the Middle Magdalena Valley, Colombia. In "Petroleum geochemistry and source rock potential of carbonate rocks" (J. G. Palacas, ed.), pp. 127-133. American Association of Petroleum Geologists, Studies in Geology 18 (1984).

[29]- Connan, J., BourouUec, J., Dessort, D., and Albrecht, P. The microbial input in carbonate-anhydrite facies of a sabkha paleoenvironment from Guatemala: A molecular approach. In "Advances in Organic Geochemistry 1985" (D. Leythaeuser and J. Rullkotter, eds.), pp. 29-50. Pergamon Press, Oxford (1986).

[30]- Prince, R. C. Hopanoids: The world's most abundant biomolecules? Trends in Biochemical Sciences 12, 455-456 (1987).

[31]- Clark, J. P., and Philp, R. P. Geochemical characterization of evaporite and carbonate depositional environments and correlation of associated crude oils in the Black Creek Basin, Alberta. Bulletin of Canadian Petroleum Geology 37, 401-416 (1989).

[32]- Mackenzie, A. S., Lamb, N. A., and Maxwell, J. R.. Steroid hydrocarbons and the thermal history of sediments. Nature 295, 223-226 (1982).

[33]- Czochanska, Z., Gilbert, T., Philp, R., Sheppard, C., Weston, R., Wood, T., and Woolhouse, A. Geochemical application of sterane and triterpane biomarkers to a description of oils from the Taranaki Basin in New Zealand. Organic Geochemistry 12, 123-135 (1988).

[34]- Grantham, P., and Wakefield, L. Variations in the sterane carbon number distributions of marine source rock derived crude oils through geological time. Organic Geochemistry 12, 61-73 (1988).

[35]- Peters, K. E., Ramos, L. S., Zumberge, J. E., Valin, Z. C., Scotese, C. R., and Gautier, D. L. Circum-Arctic petroleum systems identified using decision-tree chemometrics. American Association of Petroleum Geologists Bulletin 91, 877-913 (2007).

[36]- Seifert, W., and Moldowan, J. Use of biological markers in petroleum exploration. In "Methods in geochemistry and geophysics" (R. B. Johns), ed.), Vol. 24, pp. 261-290. Amsterdam, Elsevier (1986).

[37]- Waples, D. W., and Machihara, T. Application of sterane and tritepane biomarkers in petroleum exploration Bulletin of Canadian Petroleum Geology. Bulletin of Canadian Petroleum Geology 3, 357-380 (1990).

[38]- Philp, R. P. Formation and geochemistry of oil and gas. In "sediments, Diagenesesis, and sedemntary rocks, Treatise on Geochemistry" (F. T. Mackenzie, ed.), Vol. 7, pp. 223-256 (2007)..

[39]- ten Haven, H. L. T., Leeuw, J. W. D., Peakman, T. M., and Maxwell, J. R. Anomalies in steroid and hopanoid maturity indices. Geochimica et Cosmochimica Acta 50, 853-855 (1986).

[40]- Rullkötter, J., and Marzi, R. Natural and artificial maturation of biological markers in a Toarcian shale from northern Germany. Organic Geochemistry 13, 639-645 (1988).